Atmos. Chem. Phys. Discuss., doi:10.5194/acp-2016-591, 2016
Manuscript under review for journal Atmos. Chem. Phys.
Published: 5 September 2016


Atmospheric Chemistry and Physics Discussions
Open Access

# Air Quality Improvement in a Megacity: Implications from 2015 Beijing Parade Blue Pollution-Control Actions

Wen Xu[1#], Wei Song[2,#], Yangyang Zhang[1,#], Xuejun Liu[1,*], Lin Zhang[3], Yuanhong Zhao[3], Duanyang Liu[4], Aohan Tang[1], Daowei Yang[1], Dandan Wang[1], Zhang Wen[1], Yuepeng Pan[5], David Fowler[6], Jeffrey L. Collett Jr.[7], Jan Willem Erisman[8], Keith Goulding[9], Yi Li[10], Fusuo Zhang[1]

1. College of Resources and Environmental Sciences, Center for Resources, Environment and Food Security, Key laboratory of Plant-Soil Interactions of MOE, China Agricultural University, Beijing 100193, China
2. Institute of Surface-Earth System Science, Tianjin University, Tianjin, 300072, China
3. Laboratory for Climate and Ocean-Atmosphere Studies, Department of Atmospheric and Oceanic Sciences, School of Physics, Peking University, Beijing 100871, China
4. Jiangsu Meteorological Observatory, Nanjing 210008, China
5. State Key Laboratory of Atmospheric Boundary Layer Physics and Atmospheric Chemistry (LAPC), Institute of Atmospheric Physics, Chinese Academy of Sciences, Beijing 100029, China
6. Centre for Ecology and Hydrology Edinburgh, Bush Estate, Penicuik, Midlothian EH26 0QB, UK
7. Department of Atmospheric Science, Colorado State University, Fort Collins, CO 80523, USA
8. Louis Bolk Institute, Hoofdstraat 24, 3972 LA Driebergen, The Netherlands
9. The Sustainable Soil and Grassland Systems Department, Rothamsted Research, West Common, Harpenden, Hertfordshire, AL5 2JQ, UK
10. Arizona Department of Environmental Quality, Phoenix, AZ, 85007, USA

[#] Equal contribution; [*] Corresponding author (Email: liu310@cau.edu.cn)

**Abstract:**

The implementation of strict emission control measures in Beijing and surrounding regions during the 2015 China Victory Day Parade provided a valuable opportunity to investigate related air quality improvements in a megacity. We measured $NH_3$, $NO_2$ and $PM_{2.5}$ at multiple sites in and outside Beijing and summarized concentrations of $PM_{2.5}$, $PM_{10}$, $NO_2$, $SO_2$ and CO in 291 cities across China from a national urban air quality monitoring network between August and September 2015. Consistently significant reductions of 12-35% for $NH_3$ and 33-59% for $NO_2$ in different areas of Beijing city during the emission control period (referred to as the Parade Blue period) were observed compared with measurements in the pre- and post-Parade Blue periods without emission controls. Average $NH_3$ and $NO_2$ concentrations at sites near traffic were strongly correlated and showed positive and

Atmos. Chem. Phys. Discuss., doi:10.5194/acp-2016-591, 2016
Manuscript under review for journal Atmos. Chem. Phys.
Published: 5 September 2016


significant responses to traffic reduction measures, suggesting that traffic is an important source of both $NH_3$ and $NO_x$ in urban Beijing. Daily concentrations of $PM_{2.5}$ and secondary inorganic aerosol (sulfate, ammonium, and nitrate) at the urban and rural sites both decreased during the Parade Blue period. Concentrations of $PM_{2.5}$, $PM_{10}$, $NO_2$, $SO_2$ and CO from the national city-monitoring network showed the largest decrease (34-72%) in Beijing, a smaller decrease (1-32%) in North China (excluding Beijing), and an increase (6-16%) in other regions of China during the emission control period. Integrated analysis of modeling and monitoring results demonstrated that emission control measures made a major contribution to air quality improvement in Beijing compared with a minor contribution from favorable meteorological conditions during the Parade Blue period. These results show that controls of secondary aerosol precursors ($NH_3$, $SO_2$ and $NO_x$) locally and regionally are key to curbing air pollution in Beijing and probably in other mega cities worldwide.

## Introduction

China's economy has made great advances over the last three decades. Its gross domestic production (GDP) ranked fifteenth in the world in 1978 but has risen to second place since 2010. During this period, environmental pollution has greatly increased, including soil, water and air pollution (Chan et al., 2008; Guo et al., 2010; Chen et al., 2014; Lu et al., 2015), which has become a major issue for the country. The Chinese government and people have grown particularly concerned about reducing air pollution since the large-scale haze pollution that occurred in China in January 2013. This episode affected an area of approximately 1.3 million $km^2$ and 800 million people (Huang et al., 2014). It led to serious human health problems and forced the Chinese government to address the problem of very large exposures of the Chinese population to $PM_{2.5}$ (particulate matter $\leq$ 2.5 μm in aerodynamic diameter) pollution. For example, compared with a similar winter period without haze pollution (daily child patients < 600), more than 7000 daily child patients were

Atmos. Chem. Phys. Discuss., doi:10.5194/acp-2016-591, 2016
Manuscript under review for journal Atmos. Chem. Phys.
Published: 5 September 2016


reported in Beijing Children's Hospital during the smog period in January 2013 (http://qnck.cyol.com/html/2014-01/01/nw.D110000qnck_20140101_1-28.htm). In response to this the 'Atmospheric Pollution Prevention and Control Action Plan' was implemented by the Chinese government in September 2013, aiming to reduce $PM_{2.5}$ in Beijing by at least 25% from the 2012 level by 2017.

Many industrialized megacities have experienced severe air pollution, such as Los Angeles during the 1940s-1970s (Haagen-Smit, 1952; Parrish et al., 2011), Mexico city in the 1980s (Parrish et al., 2011), and London in the 1950s (Davis et al., 2002). In these megacities, however, enormous progress in improving air quality has been achieved with the implementation of various emission control strategies over recent decades, despite rapid population growth and urbanization. According to Parrish et al. (2011), first stage smog alerts in Los Angeles have decreased from some 200 per year in the 1970s to about 10 per year now, and concentrations of air pollutants in Mexico City have been reduced substantially over the past decades. Also, air quality is now much better in London, with mean annual $PM_{10}$ levels (particulate matter ≤10 μm in aerodynamic diameter) closer to 30 μg $m^{-3}$ than the 300 μg $m^{-3}$ fifty years ago (and approx. 3000 μg $m^{-3}$ in December 1952) (Davis et al., 2002).

Beijing, the capital of China, is one of the largest megacities in the world with 22 million inhabitants and an area of 16800 square kilometers. The city is enclosed by the Yanshan Mountains to the north and Taihang Mountains to the west. Its fan-shaped topography permits efficient southerly transport of pollutants to Beijing, which reduces air quality (Chen et al., 2015). A 70$^{th}$ anniversary victory parade was held in Beijing on 3 September 2015 to commemorate the conclusion of the second Sino-Japanese War and the end of World War II. The Chinese government imposed a series of strict and urgent air pollutant emission-reduction measures to improve air quality during what has been called the 'Parade Blue' period, from 20 August to 3 September 2015, in Beijing and surrounding regions of North China (including Tianjin, Hebei, Inner Mongolia, Shandong, Shanxi and Henan Provinces) to guarantee better air quality in the city. During this period, motor vehicles (except

Atmos. Chem. Phys. Discuss., doi:10.5194/acp-2016-591, 2016
Manuscript under review for journal Atmos. Chem. Phys.
Published: 5 September 2016


taxies and buses) with even or odd registration numbers were banned on alternate days, 1927 industrial enterprises had to limit production or were shut down, and hundreds of construction sites in Beijing were closed, reducing air pollutant emissions by 40% (http://gongyi.sohu.com/20150826/n419765215.shtml). More broadly in North China, air pollutant emissions during the Parade Blue period were decreased by 30% through a variety of reduction measures (http://news.sohu.com/20150819/n419198051.shtml). No additional pollution control measures were taken in other regions of China (outside Beijing and North China) during this period.

Previous studies have attempted to quantify the role of short-term pollutant emission control measures in air quality improvement in Beijing during the 2008 Olympics (Wang et al., 2009, 2010; Shen et al., 2011) and the 2014 Asia-Pacific Economic Cooperation (APEC) meeting (Chen et al., 2015). In addition, Tang et al. (2015) reported that local emissions are the key factors determining the formation and development of air pollution in the Beijing area. Ianniello et al. (2010) inferred that traffic may be an important emission source of $NH_3$ in Beijing. However, the above studies did not systematically answer the three following questions: what were (1) the contribution of ammonia ($NH_3$) from traffic sources to urban $PM_{2.5}$ pollution; (2) the response (linear or non-linear) of air pollutant (e.g. $PM_{2.5}$) concentrations to major pollutant emission reduction; and (3) the relative roles of pollution control measures and weather conditions in air quality improvement? The present study attempts to examine these important topics by taking advantage of the implementation of emission controls for the 70$^{th}$ anniversary victory parade. We present results showing changes in concentrations of atmospheric pollutants (i.e., $NH_3$, $NO_2$, $PM_{2.5}$ and associated inorganic water-soluble ions) before, during, and after the Parade Blue period, obtained from *in situ* measurements at thirty-one sites in and outside Beijing. In addition, we compare the Chinese Ministry of Environmental Protection officially released daily concentrations of $PM_{2.5}$, $PM_{10}$, $NO_2$, $SO_2$ and CO at 291 cities in China during the same period. The first results

Atmos. Chem. Phys. Discuss., doi:10.5194/acp-2016-591, 2016
Manuscript under review for journal Atmos. Chem. Phys.
Published: 5 September 2016


from the analysis of this extensive dataset reveal clear effects of the Parade Blue emission reduction measures on air quality improvement and provide a scientific basis for demonstrating the effectiveness of such control measures for air pollution in mega cities.

## 2 Materials and methods

### *2.1 Site selection and description*

Thirty-one air pollution monitoring sites have been established in and outside Beijing municipality, with longitudes ranging from 115.02 °E to 118.20 °E and latitudes from 36.84 °N to 40. 34 °N (**Fig. 1**). The 28 monitoring sites in Beijing municipality are grouped into road and non-road sites to better distinguish the impacts of control measures on sites near traffic. A brief description of all the sites is given below. Detailed information, including specific sampling site, site type, and potential emission sources for each site, is listed in **Table S1** in the Supplement.

*In Beijing*: Sixteen roadside monitoring sites are homogeneously distributed at the edges of three major roads, including four sites each on the 3$^{rd}$ and 4$^{th}$ ring roads, and eight sites on the 5$^{th}$ ring road. Additional road sites (sites 26 to 28) are in northwest rural regions near the Yanshan mountains. Site 26 is located at the edge of the Badaling highway, about 46 km northwest of the center of Beijing. Sites 27 and 28 are located, respectively, 100 m from the exit and 30 m from the entrance of the Badaling Highway Tunnel (1091.2 m long), which has two traffic tunnels with one lane in each. The road sites were strongly and directly influenced by vehicle emissions. Nine non-road sites were chosen over a wide area, extending from an urban area (site 1) near the city center, through suburban areas (sites 6, 11, 12 and 13) between the 3$^{rd}$ and 5$^{th}$ ring roads, and ending in rural areas (sites 22 to 25) between the northwest 5$^{th}$ and 6$^{th}$ ring roads. These are likely to be polluted by emissions from various sources, including dense housing, industry, cropland, small villages, etc.

*Outside Beijing*: Site 29 is located in a rural area of Yucheng city, Shandong province. Site 30 is located in Quzhou county, Hebei province, which is a typical

Atmos. Chem. Phys. Discuss., doi:10.5194/acp-2016-591, 2016
Manuscript under review for journal Atmos. Chem. Phys.
Published: 5 September 2016


rural agricultural site with a recently constructed industrial district. Site 31 is a regional background site located on Changdao island, Shandong province.

*2.2 Sampling procedure and sample analysis*

Atmospheric $NH_3$, $NO_2$ and $PM_{2.5}$ were measured from 3 August to 30 September 2015. The period can be divided into three phases: (1) 3-19 August (named pre-Parade Blue period), (2) 20 August-3 September (Parade Blue period), and (3) 4-30 September (post-Parade Blue period). The sampling durations, measured pollutants and number of samples for all the sites during each phase are summarized in **Table S1** in the Supplement. The measurements of $NH_3$, $NO_2$ and $PM_{2.5}$ were not concurrently made at most sites due to a shortage of manpower and samplers, but the corresponding sampling sites together covered the major emission sources of measured pollutants. Methods for sampling gases and $PM_{2.5}$ are briefly presented below. For further details of the methodology the reader is referred to relevant previous publications (Xu et al., 2014, 2015, 2016).

*Gaseous $NH_3$ and $NO_2$*: $NH_3$ samples were collected using ALPHA passive samplers (Adapted Low-cost High Absorption, provided by the Centre for Ecology and Hydrology, Edinburgh, UK) and $NO_2$ samples using Gradko diffusion tubes (Gradko International Limited, UK). At each site, three ALPHA samplers and/or three $NO_2$ tubes were deployed under a PVC shelter (2 m above the ground) to protect the samplers from rain and direct sunlight (Pictures for 4 selected road sites are shown in **Fig. S1** of the Supplement). The samplers were exposed for 7 to 14 days during the three study phases. $NH_3$ was extracted with high-purity water (18.2 MΩ) and analyzed using a continuous-flow analyzer (Seal AA3, Germany). $NO_2$ samples, also extracted with high-purity water, were analyzed using a colorimetric method by absorption at a wavelength of 542 nm. More details of the passive samplers and their laboratory preparation and analysis can be found in Xu et al. (2014, 2015).

*Airborne $PM_{2.5}$*: 24-h $PM_{2.5}$ samples were collected on 90 mm quartz fiber filters (Whatman QM/A, Maidstone, UK) using medium-volume samplers (TH-150CIII, Tianhong Co., Wuhan, China), at a flow rate of 100 L $min^{-1}$ (Xu et al., 2016). The

Atmos. Chem. Phys. Discuss., doi:10.5194/acp-2016-591, 2016
Manuscript under review for journal Atmos. Chem. Phys.
Published: 5 September 2016


$PM_{2.5}$ mass was determined using the standard gravimetric method, and one quarter of each $PM_{2.5}$ sample was ultrasonically extracted with 10 ml high-purity water for 30 min, with the extract being filtered by a syringe filter (0.45 μm, Tengda Inc., China). The water-soluble cations ($NH_4^+$, $Na^+$, $Ca^{2+}$, $K^+$, $Mg^{2+}$) and anions ($NO_3^-$, $SO_4^{2-}$, $F^-$, $Cl^-$) in the extract were analyzed using Dionex-600 and Dionex-2100 Ion Chromatographs (Dionex Inc., Sunnyvale, CA, USA), respectively (Zhang et al., 2011; Tao et al., 2014).

*2.3 Quality assurance/ Quality control (QA/QC)*

All samples were prepared and measured in the Key Laboratory of Plant-Soil Interactions, Chinese Ministry of Education, China Agricultural University, which has a complete and strict quality control system. Three field (travel) blanks were prepared for each batch of samples and analyzed together with those samples. All reported concentrations of gases and $PM_{2.5}$ mass and ion concentrations are corrected for the blanks. The detection limits were 0.01-0.02 mg $L^{-1}$ for the measured ions. The measurement precisions were in the range of 5-10% for $NH_3$, $NO_2$, $PM_{2.5}$ mass and water soluble ion concentrations. Quality assurance was routinely (once every 15-20 samples) checked using standard (designed specific concentrations of various ions) samples during sample analysis.

*2.4 Other data collection*

The 24-h (daily) average concentrations of $PM_{2.5}$, $PM_{10}$, $NO_2$, $SO_2$ and CO measured in 291 cities across China (including Beijing city, surrounding 63 cities in North China, and 227 cities in other regions of China) during the Pre-Parade Blue period and the Parade Blue period were downloaded from the Ministry of Environmental Protection (MEP) of China (http://www.mep.gov.cn). These data for each city are summarized in **Tables S2-6** in the Supplement. For Beijing city, each pollutant's daily individual Air Quality Index (AQI) during the above two periods was calculated from the 24-h average concentration. The highest individual AQI was selected and used as the daily AQI. An AQI of 0-50, 51-100, 101-150, and 151-200 is classified as “excellent”, “good”, “slightly polluted” and “moderately polluted”,

respectively. Details of the calculations of AQI and the associated classification of air quality are given in the Chinese Technical Regulations on AQI (MEPC, 2012). Daily meteorological data in the above mentioned 291 cities (1+63+227) for wind speed (WS), temperature (*T*), and relative humidity (RH) during the Parade Blue period and non-Parade Blue periods (the pre-Parade Blue period and/or the period of 8-19 September 2015) were obtained from Weather Underground (http://www.underground.com). The daily precipitation and half-hourly wind speed and direction were measured in Beijing city. The NCEP/NCAR global reanalysis meteorological data (including daily wind speed, wind direction, sea surface pressure and precipitation) during the same periods were provided by the NOAA/OAR/ESRL PSD, Boulder, Colorado, USA, from their website (http://www.esrl.noaa.gov/psd). The daily mean atmospheric mixing layer height (MLH) in Beijing during the period from 3 August to 30 September 2015 was calculated using the method described in Holzworth (1964, 1967). For Beijing city, emission reductions of major investigated variables ($PM_{2.5}$, $PM_{10}$, $NO_x$ and $SO_2$) resulting from the various control measures were uniformly assumed to be 0%, 25%, 30%, 40% and 5% during the periods 1-19 August, 20-24 August, 25-29 August, 30 August-3 September and 4-30 September 2015, respectively, because control measures began on 20 August 2015 and were more stringent during the period from 28 August to 4 September 2015 (http://china.caixin.com/2015-09-01/100845761.html). To assess the impacts of changes in pollutant emissions on resulting ambient atmospheric concentrations, a linear or nonlinear fit was performed by using the aforementioned pollutant emission reductions and the mean ambient concentrations of relevant pollutants during the five periods (averaging from officially released daily concentrations of the pollutants for Beijing city).

*2.5 Back trajectories and statistical analysis*

The 72-h (3-day) backward trajectories arriving at Beijing were calculated four times a day (00:00, 06:00, 12:00, and 18:00 UTC) at 100 m height using the Hybrid Single

Atmos. Chem. Phys. Discuss., doi:10.5194/acp-2016-591, 2016
Manuscript under review for journal Atmos. Chem. Phys.
Published: 5 September 2016


Particle Lagrangian Integrated Trajectory (HYSPLIT-4, NOAA) 4.9 model (Draxler and Hess, 1997). Meteorological data with a resolution of 0.5° × 0.5° were input from the Global Data Assimilation System (GDAS) meteorological data archives of the Air Resource Laboratory, National Oceanic and Atmospheric Administration (NOAA). The trajectories were then grouped into four clusters during each period using cluster analysis based on the total spatial variance (TSV) method (Draxler et al., 2012). Values of $NH_3$, $NO_2$, $PM_{2.5}$ and ion concentrations per study phase at the sampling sites are shown as the mean ± standard error (SE). Temporal differences between study phases of concentrations of measured gases ($NH_3$ and $NO_2$) and the MEP of reported pollutants (i.e. $PM_{2.5}$, $PM_{10}$, $NO_2$, $SO_2$ and CO) were investigated using paired t-tests while those of measured $PM_{2.5}$ mass and associated ionic components were investigated using a non-parametric Mann-Whitney U test. All statistical analyses were performed using SPSS11.5 (SPSS Inc., Chicago, IL, USA). Statistically significant differences were set at $p < 0.05$ unless otherwise stated.

## 3. Results

### *3.1 Concentrations of gaseous $NH_3$ and $NO_2$*

Ambient $NH_3$ concentrations varied greatly during the pre-Parade Blue, Parade Blue and post-Parade Blue periods, with values of 8.2-31.7, 7.8-50.7 and 7.4-40.2 μg $m^{-3}$, respectively (**Fig. 2A a**). The average $NH_3$ concentrations during the three periods for the sites within the 6$^{th}$ ring road (abbreviated as SWR, including road sites (RS) on the 3$^{rd}$, 4$^{th}$ and 5$^{th}$ ring roads and non-road sites (NRS)), outside the 6$^{th}$ ring road but in Beijing (SOI) and outside Beijing (SOB), are shown in **Fig. 2A b and c**. The mean $NH_3$ concentration at SWR was significantly smaller (by 13%) during the Parade Blue period compared with the mean during the post-Parade Blue period (20.2 ± 1.2 μg $m^{-3}$ versus 23.3 ± 1.8 μg $m^{-3}$); further, on all three ring roads reductions (23 to 35%) of the mean during the Parade Blue period were statistically significant while at the NRS a small non-significant increase (15%) in the mean was observed (**Fig. 2A c**). The mean $NH_3$ concentration at SOI was 12% smaller in the

Atmos. Chem. Phys. Discuss., doi:10.5194/acp-2016-591, 2016
Manuscript under review for journal Atmos. Chem. Phys.
Published: 5 September 2016


Parade Blue period than in the post-Parade Blue period (21.4 ± 6.0 μg $m^{-3}$ versus 24.3 ± 9.3 μg $m^{-3}$), whereas at SOB, non-significant increases (on average 80%) in the mean occurred during the Parade Blue period (26.7 ± 12.6 μg $m^{-3}$) compared with those during the pre- and post-Parade Blue periods (19.9 ± 6.2 and 11.8 ± 2.3 μg $m^{-3}$, respectively).

Ambient $NO_2$ concentrations ranged from 21.5 to 227.7, 14.1 to 258.8, and 15.7 to 751.8 μg $m^{-3}$ during the pre-Parade Blue, Parade Blue and post-Parade Blue periods, respectively (**Fig. 2B a**). The mean $NO_2$ concentrations at SWR (including road sites on the 5th ring road and NRS), SOI and SOB during the three periods are shown in **Fig. 2B b and c**. At SWR, the mean concentration during the Parade Blue period (78.7 μg $m^{-3}$) was 42% and 35% lower ($p$<0.01) than the means during the pre- and post-Parade Blue periods (135.7 ± 21.8 and 121.0 ± 16.5 μg $m^{-3}$, respectively). For the 5th ring road sites and NRS, most reductions (33~42%) in the mean during the Parade Blue period were also highly significant ($p$<0.01). At SOI, a large non-significant reduction (59%) in the mean concentration occurred during the Parade Blue period compared with the post-Parade Blue period (183.5 ± 49.1 versus 443.4 ± 173.3 μg $m^{-3}$). At SOB, the change in the mean during the Parade Blue period (23.7 ± 3.6 μg $m^{-3}$) was small and non-significant when compared with the means during the pre- and post-Parade periods (27.5 ± 4.5 and 18.5 ± 1.7 μg $m^{-3}$, respectively).

### *3.2 Concentrations of $PM_{2.5}$ and its chemical components*

A statistical analysis of concentrations of $PM_{2.5}$ mass and associated WSIs at sites 22, 29 and 30 in the three periods is presented in **Table 1**. Daily $PM_{2.5}$ concentrations ranged from 4.2 to 123.6, 15.4 to 116.0, and 12.4 to 170.7 μg $m^{-3}$ at sites 22, 29 and 30, respectively. At sites 22 and 29, mean $PM_{2.5}$ concentrations during the Parade Blue period decreased significantly (by 49% and 40%, respectively) compared with the means during the pre-Parade Blue period, and increased again during the post-Parade Blue period (57% and 3%, respectively) compared with the means

Atmos. Chem. Phys. Discuss., doi:10.5194/acp-2016-591, 2016
Manuscript under review for journal Atmos. Chem. Phys.
Published: 5 September 2016


during the Parade Blue period. At site 30, a 24% reduction in mean $PM_{2.5}$ concentrations occurred during the Parade Blue period compared with the pre-Parade Blue period and a 103% increase during the post-Parade Blue period.

Secondary inorganic aerosols (SIA) (sum of $NH_4^+$, $NO_3^-$ and $SO_4^{2-}$) were major components of $PM_{2.5}$, with average contributions of 24%, 41% and 32% to the daily average $PM_{2.5}$ mass at sites 22, 29 and 30, respectively. As with $PM_{2.5}$ concentrations, concentrations of all the WSIs (except for $Cl^-$) at site 22 decreased significantly during the Parade Blue period compared with the pre- and/or post-Parade Blue periods. Analogous behavior also occurred at sites 29 and 30 for concentrations of $NO_3^-$, $NH_4^+$ and $SO_4^{2-}$ but not for those of most of other ions (e.g. $Ca^{2+}$, $K^+$, $F^-$, $Na^+$).

*3.3 Daily mean pollutant concentrations from MEP*

Daily mean concentrations of the five major pollutants ($PM_{2.5}$, $PM_{10}$, $NO_2$, $SO_2$ and CO) at 291 cities in China, divided into three groups of Beijing, cities in North China (NC, area surrounding Beijing) and cities in other regions of China, are summarized in **Fig. 3**. Average concentrations of $PM_{2.5}$, $PM_{10}$, $NO_2$, $SO_2$ and CO during the Parade Blue period were highly significantly ($p$<0.01) decreased in Beijing, with reductions of 72%, 67%, 39%, 34% and 39%, respectively, compared with the pre-Parade Blue period. $PM_{2.5}$ concentrations in Beijing, for example, remained below 20 μg $m^{-3}$ for 14 consecutive days in the Parade Blue period (for comparison: the WHO and China's (first-grade) thresholds for daily $PM_{2.5}$ concentrations are 25 and 35 μg $m^{-3}$, respectively). The daily $PM_{2.5}$ concentrations in Beijing in the pre-Parade Blue period averaged 59 μg $m^{-3}$. Concentrations of $PM_{2.5}$, $PM_{10}$ and $SO_2$ in the Parade Blue period were also significantly ($p$<0.05) decreased in cities in north China (excluding Beijing), with reductions of 32%, 29% and 7%, respectively, while concentrations of $NO_2$ and CO did not show statistically significant changes ($p$>0.05). In cities in other regions, by contrast, where no additional emission reduction measures were taken, concentrations of $PM_{2.5}$, $PM_{10}$,

Atmos. Chem. Phys. Discuss., doi:10.5194/acp-2016-591, 2016
Manuscript under review for journal Atmos. Chem. Phys.
Published: 5 September 2016


$NO_2$, $SO_2$ and CO remained stable or were significantly ($p$<0.05) higher during the Parade Blue period compared with the pre-Parade Blue period.

## 4. Discussion

### *4.1 Effect of emission controls on air quality*

The statistical analyses (**Fig. 3**) show that, by taking regional emission controls during the Parade Blue period, daily concentrations of the five reported pollutants ($PM_{2.5}$, $PM_{10}$, $NO_2$, $SO_2$ and CO) in Beijing city and other cities in North China were decreased by various but statistically significant amounts, in sharp contrast to increases in cities in other parts of China where no additional emission controls were imposed. This shows the effectiveness of the pollution controls and suggests that air quality improvement was directly related to the reduction intensities of pollutant emissions (e.g., air pollution control effects ranked by Beijing (largest reduction) > North China (moderate reduction) > other regions (no reduction) in China). Another way of quantifying the effect of the additional control measures for Beijing uses the Air Quality Index (MEPC, 2012). On the basis of the calculated air quality index (AQI, **Fig. 5**), 89% for the days of the pre-Parade Blue period were classified as "good", and the primary pollutant was $PM_{2.5}$ for 82% of these days. In contrast, almost all of the days during the Parade Blue period were defined as "excellent". Thus improved air quality-as represented by the AQI during the Parade Blue period was mainly attributed to the additional control of $PM_{2.5}$ precursors.

Results from the MEP of source apportionment of $PM_{2.5}$ for Beijing (http://www.bj.xinhuanet.com/bjyw/2014-04/17/c_1110289403.htm) showed that 64-72% of atmospheric $PM_{2.5}$ during 2012-2013 was generated by emissions from local sources, of which the biggest contributor was vehicle exhaust (31.1%), followed by coal combustion (22.4%), industrial production (18.1%), soil dust (14.3%) and others (14.1%). The contribution from vehicles had increased by 1.7 percentage points compared to 2010-2011. To examine the contribution of vehicles, power plants, and industries to $PM_{2.5}$ concentrations, $PM_{2.5}$ concentrations from

Atmos. Chem. Phys. Discuss., doi:10.5194/acp-2016-591, 2016
Manuscript under review for journal Atmos. Chem. Phys.
Published: 5 September 2016


these were compared with those of other primary pollutants such as $NO_x$ ($NO+NO_2$), CO and $SO_2$ (Zhao et al., 2012). As shown in **Fig. S2a-d** in the Supplement, the linear correlations of $PM_{2.5}$ with each pollutant gas (CO, $NO_2$ and $SO_2$) and their sum were positive and highly significant (R=0.50-0.88, $p<0.05$) during the study period, except for the relationship between $PM_{2.5}$ and $NO_2$ during the pre-Parade Blue period and that of $PM_{2.5}$ versus $SO_2$ during the Parade Blue period, both of which were positive but not significant ($p>0.05$). This finding is consistent with the source apportionment results that suggest traffic, power plants and industry are significant sources of $PM_{2.5}$ in Beijing. Given the importance of local vehicle emissions vs. more distant power plant and industrial emissions for Beijing's air quality, the ratio of $CO/SO_2$ can be used as an indicator of the contribution of local emissions to air pollution, with higher ratios indicating higher local contributions (Tang et al., 2015). Ratios of $CO/SO_2$ decreased (on average by 22%) from the pre-Parade Blue to Parade Blue period (**Fig. 5**), further suggesting the decreased amount of pollutants from local contributions. Beijing has relatively little industry but numerous automobiles, and the emissions of $SO_2$ are small while those of CO and $NO_x$ are much larger (Zhao et al., 2012). Thus, traffic emission is likely to be a determining factor influencing urban CO and $NO_x$ levels. This, in combination with a strong positive and highly significant correlation of $PM_{2.5}$ versus $CO+NO_2$ during the study period (**Fig. S2e, Supplement**), and the weak correlation of $PM_{2.5}$ versus $SO_2$ noted above (**Fig. S2c, Supplement**), shows that traffic emission controls should be a priority in mitigating $PM_{2.5}$ pollution in the future.

Concentrations of $PM_{2.5}$ levels in Beijing are not only driven by primary emissions but are also affected by meteorology and atmospheric chemistry operating on the primary pollutants, leading to secondary pollutant formation (Zhang et al., 2015). To quantify the likely contribution of secondary pollutant formation of $PM_{2.5}$ as a contributor to the observed changes between the Parade Blue period and pre- and post-measurements, CO provides an excellent tracer for primary combustion sources (de Gouw et al., 2009). Daily ratios of $PM_{2.5}$/CO decreased (by 50%) significantly

Atmos. Chem. Phys. Discuss., doi:10.5194/acp-2016-591, 2016
Manuscript under review for journal Atmos. Chem. Phys.
Published: 5 September 2016


during the Parade Blue period compared with those during the pre-Parade Blue period (**Fig. 5**), which suggests that the significant reduction of $PM_{2.5}$ concentrations during the Parade Blue period was not only due to less anthropogenic primary emissions but also due to reduced secondary pollutant formation. This is further supported by our measured results at urban site 22, where average SIA concentrations comprised 20-29% of average $PM_{2.5}$ mass over the three periods, and decreased significantly during the Parade Blue period compared with those during the pre- and post-Parade Blue periods (**Table 1**). Significant reductions of concentrations of precursor gases (e.g. $NO_2$, $SO_2$ and $NH_3$) at the city scale is likely to be the major reason for such reduced secondary pollutant formation. In addition, lower concentrations of sulfate and nitrate during the Parade Blue period might also be caused by lower oxidation rates of $SO_2$ and $NO_x$. The sulfur oxidation ratio ($SOR=nSO_4^{2-}/(nSO_4^{2-}+nSO_2)$) and the nitrogen oxidation ratio ($NOR=nNO_3^-/(nNO_3^-+nNO_2)$) ($n$ refers to the molar concentration) are indicators of secondary pollutant transformation in the atmosphere. Higher values of SOR and NOR imply more complete oxidation of gaseous species to sulfate- and nitrate-containing secondary particles (Sun et al., 2006). To understand the potential change in the degree of oxidation of sulfur and nitrogen, we used daily concentrations of $SO_4^{2-}$ and $NO_3^-$ measured at urban site 22 (located at west campus of China Agricultural University) and the MEP-reported concentrations of $SO_2$ and $NO_2$ at the Wanliu monitoring station to calculate the SOR and NOR values. This is because these two sites, only 7 km apart (**Fig. S3, Supplement**), experience similar pollution climates. The average values of SOR and NOR were 0.64 and 0.04 during the pre-Parade Blue period, and 0.47 and 0.03 during the Parade Blue period (**Fig. S4, Supplement**). Slightly reduced values of SOR and NOR from the pre-Parade Blue to Parade Blue periods suggests a possible minor role for changes in the extent of photochemical oxidation in secondary transformation.

Ammonia is the primary alkaline trace gas in the atmosphere. In ammonia-rich environments, $NH_4HSO_4$ and $(NH_4)_2SO_4$ are sequentially formed, and the surplus

Atmos. Chem. Phys. Discuss., doi:10.5194/acp-2016-591, 2016
Manuscript under review for journal Atmos. Chem. Phys.
Published: 5 September 2016


$NH_3$ that does not react with $H_2SO_4$ can form $NH_4NO_3$ (Wang et al., 2005). In both the pre-Parade Blue and Parade Blue periods, $NH_4^+$ was strongly correlated with $SO_4^{2-}$ (**Fig. S5 a** and **c, Supplement**) and [$SO_4^{2-}$+$NO_3^-$] (**Fig. S5 b** and **d, Supplement**), and the regression slopes were both 0.87 during the pre-Parade Blue period, and 0.97 and 0.91, respectively, during the Parade Blue period. These results indicate almost complete neutralization of acidic species ($HNO_3$ and $H_2SO_4$) by $NH_3$ in $PM_{2.5}$ during these two periods especially in the Parade Blue period. In this way, SIA concentrations from these sources could not be further reduced during the Parade Blue period unless $NH_3$ emissions were reduced more than those of $SO_2$ and $NO_x$.

*4.2 Impact of traffic $NH_3$ emission on urban $NH_3$ concentration*

The sources of $NH_3$ are dominated by agriculture, but it may also be produced by motor vehicles due to the over-reduction of NO in catalytic converters (Kean et al., 2000). The contribution of traffic to the total $NH_3$ emissions is estimated at approximately 2% in Europe (EEA, 2011) and 5% in the US (Kean et al., 2009). In China, $NH_3$ emissions from traffic rose from 0.005 Tg (contributing approximately 0.08% to total $NH_3$ emissions) in 1980 to 0.5 Tg (contributing approximately 5% to total emissions) in 2012 (Kang et al., 2016). Traffic is therefore likely to make a very significant contribution to $NH_3$ concentrations in urban areas of Beijing, and a strong correlation of $NH_3$ with traffic-related pollutants was observed ($NO_x$ and CO) at the urban sites (Ianniello et al., 2010; Meng et al., 2011). However, this relationship has a large uncertainty because the concentrations of pollutants used to establish the relationship were measured at 'background' urban sites some distance from major roads, and other urban sources such as decaying organic matter may contribute. In the present study, strong and significant correlations were observed between $NH_3$ and $NO_2$ concentrations measured on the 5$^{th}$ ring road during all three periods (**Fig. 6**). In addition, compared with the averages for the three ring roads during the pre- and/or post-Parade Blue periods, the average $NH_3$ concentrations during the Parade Blue period decreased significantly owing to traffic reduction

measures (**Fig. 2A c**). These results provide strong evidence that traffic is an important source of $NH_3$ in Beijing. In addition to period-to-period temporal changes, the mean $NH_3$ concentration at all road sites was 1.3 and 1.9 times that at all non-road sites during the Parade Blue period and post-Parade Blue period, respectively (**Fig. 2A**). Moreover, during the post-Parade Blue period the measured $NH_3$ concentrations on the three ring roads (28.3 ± 6.4 μg $m^{-3}$) were twice those at the rural sites 29 and 30 (14.0 ± 1.6 μg $m^{-3}$) affected by intense agricultural $NH_3$ emissions. These results, along with the fact that urban Beijing has a higher relative on-road vehicle density and almost no agricultural activity, suggest that $NH_3$ emission and transport from local traffic were the main contributors to high urban $NH_3$ concentrations. Based on a mileage-based $NH_3$ emission factor of 230 ± 14.1 mg $km^{-1}$ for light-duty gasoline vehicles (Liu et al., 2014), a population of 5.61 million vehicles (average mileage 21849 km $vehicle^{-1}$ $yr^{-1}$) in Beijing would produce approximately 28 kt $NH_3$ in 2015, which likely declined by up to 38 t $NH_3$ $day^{-1}$ during the Parade Blue period, given that the traffic load decreased by half with the implementation of the odd-and-even car ban policy.

*4.3 Impact of meteorological conditions and long-range air transport*

Meteorological conditions strongly regulate near-surface air pollutant concentrations (Liu et al., 2015), contributing the largest uncertainties to the evaluation of the effects of emission controls on pollutant reduction. Here we first compared the meteorological data obtained during the Parade Blue period with those from the pre- and/or post-Parade Blue periods in Beijing and other cities over North China. In Beijing, neither wind speed (WS) nor relative humidity (RH) differed significantly between non-Parade Blue (the pre- and post-Parade Blue) and the Parade Blue periods, while temperature (*T*) showed a significant but small decrease with time (**Fig. 7**). Similarly, there were small and non-significant changes in *T*, WS and RH between the pre-Parade Blue and Parade Blue periods for North China and for other cities in China. These results suggest that the period-to-period changes in *T*, WS and

Atmos. Chem. Phys. Discuss., doi:10.5194/acp-2016-591, 2016
Manuscript under review for journal Atmos. Chem. Phys.
Published: 5 September 2016


RH may have only a minor impact on $PM_{2.5}$, $PM_{10}$, $NO_2$, $SO_2$ and CO concentrations in the emission control regions (**Fig. 3**). In contrast, a higher temperature during the Parade Blue period, compared to the post-Parade Blue period, can in part explain the corresponding higher $NH_3$ concentrations measured at NRS, due to increased $NH_3$ emissions from biological sources such as humans, sewage systems and organic waste in garbage containers (Reche et al., 2012).

Surface weather maps of China and North China (**Figs. 8 and 9**) showed an apparent change of wind field over Beijing and North China during the Parade Blue period compared with the other two periods. As shown in **Fig. 9**, Beijing was located at the rear of a high pressure system within the southeast/south flow or in a high-pressure area when the wind was weak (<3 m $s^{-1}$), and at the base of the Siberian high pressure system when influenced by a weak cold front and easterly wind (> 4 m $s^{-1}$) in the non-Parade (pre- or post-Parade) Blue and Parade Blue periods, respectively. The former weather condition (non-Parade Blue periods) was conducive to pollutant convergence and the latter (Parade Blue period) was conducive to pollutant dispersion. A further analysis of wind rose plots (**Fig. 10a**) showed that northerly winds, with similar wind speeds, dominated all three periods. Northerly/northwesterly winds in Beijing bring relatively clean air due to a lack of heavy industry in the areas north/northwest of Beijing. Winds during the pre- and post-Parade Blue periods were occasionally from the south, southeast and east of Beijing, where the regions (e.g. Hebei, Henan and Shandong provinces) are characterized by substantially higher anthropogenic emissions of air pollutants such as $NH_3$, $NO_x$, $SO_2$ and aerosols (Zhang et al., 2009; Gu et al., 2012). Also as mentioned earlier, the topography of the mountains to the West and North of Beijing effectively traps the polluted air over Beijing during southerly airflow, suggesting that the southerly wind during non-Parade Blue periods may enhance air pollution in Beijing. Wet scavenging from precipitation, although often important in summer (Yoo et al., 2014), probably played a minor role in changing the concentrations of pollutants given the low and comparable precipitation over Beijing and surrounding

areas during the study periods (**Fig. 8**). For example, the total precipitation in Beijing was comparable between the pre-Parade Blue and Parade Blue periods (38.9 versus 34.4 mm) (**Fig. 10b**). In addition, we compared daily mean mixing layer height (MLH) in Beijing during the study period (**Fig. 11a**). The daily mean MLH in Beijing was approx. 37% higher during the Parade Blue period (1777 m) than the pre-Parade (1301 m) and post-Parade (1296 m) Blue periods (**Fig. 11b**, $p$ = 0.08). Since the MLH during Parade Blue was higher than that during non-Parade Blue periods, the horizontal and vertical diffusion conditions during the Parade Blue period were better than the other two periods.

Changes in meteorological conditions often lead to changes in regional pollution transport and ventilation. It has been shown that regional transport from neighboring Tianjin, Hebei, Shanxi, and Shandong Provinces can have a significant impact on Beijing's air quality (Meng et al., 2011; Zhang et al., 2015). Model calculations by Zhang et al. (2015) suggested that about half of Beijing's $PM_{2.5}$ pollution originates from sources outside of the city. Trajectory analysis in previous studies revealed that the air mass from south and southeast regions of Beijing led to high concentrations of $NH_3$, $NO_x$, $PM_{2.5}$ and secondary inorganic ions during summertime (Ianniello et al., 2010; Wang et al., 2010; Sun et al., 2015). The 72-hour back trajectories during the three measurement periods, shown in **Fig. 4**, were classified into 4 sectors according to air mass pathways: the west pathway over southern Mongolia, western Inner Mongolia, and SinKiang, the north pathway over Inner Mongolia, Heilongjiang and north Hebei Provinces, the east pathway mainly over northeast Hebei province and Tianjin municipality, and the south sector over the south Hebei and Shandong provinces. The results indicated that transport of regional pollution from the south sector occurred during the pre-Parade Blue period (38%) and the post-Parade Blue period (18% for $PM_{2.5}$ sampling days and 29% for $NH_3$ sampling days) but there was no transport of regional pollution during the Parade Blue period. As the south of Hebei province contains heavily polluting industry and intensive agriculture (Zhang et al., 2009; Sun et al., 2015), the absence of transport of air

Atmos. Chem. Phys. Discuss., doi:10.5194/acp-2016-591, 2016
Manuscript under review for journal Atmos. Chem. Phys.
Published: 5 September 2016


masses from the south sector is likely at least partly responsible for lower concentrations of the five reported pollutants ($PM_{2.5}$, $PM_{10}$, $NO_2$, $SO_2$ and CO) during the Parade Blue period. As for $NH_3$, however, average concentration at NRS were slighter higher in the Parade Blue period than in the post-Parade Blue period (**Fig. 2A c**), indicating that surface levels of $NH_3$ were less influenced by southern air masses. Much of the airflow travelled over Tianjin municipality during the Parade Blue period (32%) compared to that during the post-Parade Blue period (19%) (**Fig. 4 b**, **d**), which probably caused the high surface $NH_3$ concentrations in Beijing. This is because Tianjin, as one of the mega-cities in China, has high $NH_3$ emissions from livestock and fertilizer application (Zhang et al., 2010).

To further diagnose the impacts of meteorology on the surface air quality, we conducted a simulation using the nested GEOS-Chem atmospheric chemistry model driven by the GEOS-FP assimilated meteorological fields at 1/4°×5/16° horizontal resolution (Zhang et al., 2015). By fixing anthropogenic emissions in the simulation, the model provides a quantitative estimate of the meteorological impacts alone. Model results showed that, without emission controls, the air pollutant concentrations at Beijing in the Parade Blue period relative to the pre-Parade period would be 29% lower for $PM_{2.5}$, 7% lower for $NH_3$, 17% lower for $SO_2$, 8% lower for CO and relatively no change for $NO_2$ (**Fig. 12a**), which can be attributed to the different meteorological conditions as discussed above. Compared with meteorological condition changes (MCC), air pollution control measures (PCM) made a greater contribution to air quality improvement (especially for $PM_{2.5}$, $NO_x$, and CO) in Beijing during the Parade Blue period (**Fig. 12b**). Daily mean concentrations of $PM_{2.5}$ and $PM_{10}$, $NO_2$ and $SO_2$ appeared to decrease nonlinearly ($PM_{2.5}$ and $PM_{10}$) or linearly ($NO_2$ and $SO_2$) as a function of their respective pollutant emission reductions (**Fig. 13**). This is because ambient particulate matter (including $PM_{2.5}$ and $PM_{10}$) levels relative to ambient $NO_x$ and $SO_2$ levels, were affected not only by emission sources but also by secondary aerosol formation, meteorological conditions and regional atmospheric transport (Sun et al., 2016).

Atmos. Chem. Phys. Discuss., doi:10.5194/acp-2016-591, 2016
Manuscript under review for journal Atmos. Chem. Phys.
Published: 5 September 2016


*4.4 Implications for regional air pollution control*

Besides Tianjin, Beijing city is surrounded by four provinces, Hebei, Shandong, Henan and Shanxi, which all have major power plants and manufacturing industry. In the INTEX-B emission inventory, the total emissions from these four provinces accounted for 28.7%, 27.9%, 28.3%, and 25.0% of national emissions of $PM_{2.5}$, $PM_{10}$, $SO_2$, and $NO_x$, respectively (Zhang et al., 2009). The 'Parade Blue' experience demonstrates that, by taking appropriate but strict coordinated regional and local emission controls, air quality in megacities can be significantly and quickly improved. Nevertheless, we observed nonlinear relationships between emission reductions and ambient $PM_{2.5}$ and $PM_{10}$ levels, which were closely linked to variations of meteorological conditions and regional transport, suggesting that long-term and stricter regional emission controls are necessary for sustainable continuous improvement in air quality in megacities.

China is not the first country to use temporal emission control strategies. In 1996, the city of Atlanta, for example, adopted a series of actions to reduce traffic volume and significantly improved air quality during the Atlanta Olympic Games (Tian and Brimblecombe, 2008; Peel et al., 2010). We also should note that most of these emission control strategies have not been maintained after the Olympic Games. In the long term, temporary emission control strategies will not improve regional air quality conditions and we should seek better ways towards sustainable development. Integrated emission reduction measures are therefore necessary, but meteorological conditions also need to be considered for a sustainable solution, as in Urumqi, northwest China (Song et al., 2015). We therefore recommend further efforts to build on the Parade Blue experience of successful air quality improvement in Beijing and North China to improve air pollution control policies throughout China and in other rapidly developing countries.

Chinese national $SO_2$ emissions have been successfully reduced by 14% from the 2005 level due to an $SO_2$ control policy (Wang et al., 2014), and nationwide controls

on $NO_x$ emissions have been implemented along with the controls on $SO_2$ and primary particles during 2011-2015. However, there is as yet no regulation or policy that targets national $NH_3$ emissions. Future emission control policies to mitigate PM and SIA pollution in China should, in addition to focusing on primary particles, $NO_x$ and $SO_2$, also address $NH_3$ emission reduction from both agricultural and non-agricultural sectors (e.g. traffic sources) in particular when $NH_3$ becomes key to $PM_{2.5}$ formation.

## Conclusions

We have presented atmospheric concentrations of $NH_3$, $NO_2$, $PM_{2.5}$ and associated inorganic water-soluble ions before, during, and after the Parade Blue period measured at thirty-one *in situ* sites in and outside Beijing, and daily concentrations of $PM_{2.5}$, $PM_{10}$, $NO_2$, $SO_2$ and CO in 291 cities in China during the pre-Parade Blue and Parade Blue periods released by the Ministry of Environmental Protection (MEP) of China. Our unique study examines temporal variations at local and regional scales across China and the relative role of the emission controls and meteorological conditions, as well as the contribution of traffic, to $NH_3$ levels in Beijing based on the first direct measurements of $NH_3$ and $NO_2$ concentrations at road sites. The following major findings and conclusions were reached:

The concentrations of $NH_3$ and $NO_2$ during the Parade Blue period at the road sites in different areas of Beijing decreased significantly by 12-35% and 34-59% respectively relative to the pre-and post-Parade Blue measurements, while those at the non-road sites showed an increase of 15% for $NH_3$ and reductions of 33% and 42% for $NO_2$. Positive and significant correlations were observed between $NH_3$ and $NO_2$ concentrations measured at road sites. Taken together, these findings indicate that on-road traffic is an important source of $NH_3$ in the urban Beijing. Daily concentrations of $PM_{2.5}$ and secondary inorganic aerosols (sulfate, ammonium, and nitrate) at the urban and rural sites both decreased during the Parade Blue period,

which was closely related to controls of secondary aerosol precursors ($NH_3$, $SO_2$ and $NO_x$) and/or reduced secondary pollutant formation.

During the Parade Blue period, daily concentrations of air pollutants ($PM_{2.5}$, $PM_{10}$, $NO_2$, $SO_2$ and CO) in 291 cities obtained from the national air quality monitoring network showed large and significant reductions of 34-72% in Beijing, small reductions of 1-32% in cities of North China (excluding Beijing), and slight increases (6~16%) in other cities outside North China that in some cases were significant, which reflects the positive effects of emission controls on air quality and suggests that the extent of air quality improvement was directly associated with the reduction intensities of pollutant emissions.

A detailed characterization of meteorological parameters and regional transport demonstrated that the good air quality in Beijing during the Parade Blue period was the combined result of emission controls, meteorological effects and the absence of transport of air masses from the south of Beijing. Thus, the net effectiveness of emission controls was investigated further by excluding the effects of meteorology in model simulations, which showed that emission controls can contribute reductions of pollutant concentrations of nearly 60% for $PM_{2.5}$, 109% for $NO_2$, 80% for CO, 53% for $NH_3$ and 50% for $SO_2$. This result showed that emission controls played an dominant role in air quality improvement in Beijing during the Parade Blue period.

**Acknowledgments**

We thank L. Lu, T.X. Hao, S. Wang and W. Wang for their assistance during the field measurements. This work was financially supported by the China National Funds for Distinguished Young Scientists (Grant 40425007) and the innovative group grant of NSFC (Grant 31421092).

**Author Contributions**

X.L. and F.Z. designed the research. X.L., W.X., W.S., Y.Z., D.Y., D.W. Z.W. and A.T. conducted the research (collected the data and performed the measurements).

W.X., W.S. and X.L. wrote the manuscript. All authors were involved in the discussion of the study and D.F., J.L.C, K.G., J.W.E., L.Z. and Y.P. commented on the manuscript and interpretation of the data.

## References

Chan, C. K., and Yao, X. H.: Air pollution in mega cities in China. Atmos. Environ., 42, 1-42, doi:10.1016/j.atmosenv.2007.09.003, 2008.

Chen, C., Sun, Y. L., Xu, W. Q., Du, W., Zhou, L. B., Han, T. T., Wang, Q. Q., Fu, P. Q., Wang, Z. F., Gao, Z. Q., Zhang, Q., and Worsnop, D. R.: Characteristics and sources of submicron aerosols above the urban canopy (260 m) in Beijing, China, during the 2014 APEC summit, Atmos. Chem. Phys., 15, 12879-12895, doi:10.5194/acp-15-12879-2015, 2015.

Chen, R. S., De Sherbinin, A., Ye, C., and Shi, G. Q.: China's Soil Pollution: Farms on the Frontline, Science, 344, 691-691, 2014.

Davis, D. L., Bell, M. L., and Fletcher, T.: A Look Back at the London Smog of 1952 and the Half Century Since, Environ. Health Persp., 110, A734-A735, 2002.

de Gouw, J. A., Welsh-Bon, D., Warneke, C., Kuster, W. C., Alexander, L., Baker, A. K., Beyersdorf, A. J., Blake, D. R., Canagaratna, M., Celada, A. T., Huey, L. G., Junkermann, W., Onasch, T. B., Salcido, A., Sjostedt, S. J., Sullivan, A. P., Tanner, D. J., Vargas. O., Weber, R. J., Worsnop, D. R., Yu, X. Y., and Zaveri, R.: Emission and chemistry of organic carbon in the gas and aerosol phase at a sub-urban site near Mexico City in March 2006 during the MILAGRO study, Atmos. Chem. Phys., 9, 3425-3442, 2009.

Draxler, R. R., and Hess, G.: Description of the HYSPLIT4 modeling system, Air Resources Laboratory, Silver Spring, Maryland,1997.

Draxler, R., Stunder, B., Rolph, G., Stein, A., and Taylor, A.: HYSPLIT4 user's guide, version 4, report, NOAA, Silver Spring, Md, 2012.

EEA (European Environment Agency): Air Quality in Europe-2011 Report, Technical Report 12/2011, EEA, Kopenhagen, 2011.

Gu, B. J., Ge, Y., Ren, Y., Xu, B., Luo, W. D., Jiang, H., Gu, B. H., and Chang, J.: Atmospheric reactive nitrogen in China: Sources, recent trends, and damage costs. Environ. Sci. Technol., 46, 9240-9247, doi:10.1021/es301446g, 2012.

Guo, J. H., Liu, X. J., Zhang, Y., Shen, J. L., Han, W. X., Zhang, W. F., Christie, P., Goulding, K., Vitousek, P., Zhang, F. S.: Significant soil acidification in major Chinese croplands, Science, 327, 1008-1010, doi: 10.1126/science.1182570, 2010.

Haagen-Smit, A.J.: Chemistry and physiology of Los Angeles smog, Ind. Eng. Chem., 44, 1342-1346, doi:10.1021/ie50510a045, 1952.

Holzworth, G. C.: Estimates of mean maximum mixing depths in the contiguous United States, Monthly Weather Review, 92, 235-242, 1964.

Holzworth, G. C.: Mixing depths, wind speeds and air pollution potential for selected locations in the United States, Journal of Applied Meteorology, 6,1039-1044, 1967.

Huang, R.-J., Zhang, Y., Bozzetti, C., Ho, K.-F., Cao, J.-J., Han, Y., Daellenbach, K. R., Slowik, J. G., Platt, S. M., Canonaco, F., Zotter, P., Wolf, R., Pieber, S. M., Bruns, E. A., Crippa, M., Ciarelli, G., Piazzalunga, A., Schwikowski, M., Abbaszade, G., Schnelle-Kreis, J., Zimmermann, R., An, Z., Szidat, S., Baltensperger, U., Haddad, I. E., and Prevot, A. S. H.: High secondary aerosol contribution to particulate pollution during haze events in China, Nature, 514, 218-222, 2014.

Ianniello, A,, Spataro, F,, Esposito, G,, Allegrini, I,, Rantica, E,, Ancora, M. P., Hu, M., and Zhu, T.: Occurrence of gas phase ammonia in the area of Beijing (China), Atmos. Chem. Phys., 10, 9487-9503, doi:10.5194/acp-10-9487-2010, 2010.

Kang, Y. N., Liu, M. X., Song, Y., Huang, X., Yao, H., Cai, X. H., Zhang, H. S., Kang, L., Liu, X. J., Yan, X. Y., He, H., Zhang, Q., Shao, M., and Zhu, T.: High-resolution ammonia emissions inventories in China from 1980 to 2012, Atmos. Chem. Phys., 16, 2043-2058, doi: 10.5194/acp-16-2043-2016, 2016.

Kean, A. J., and Harley, R. A.: On-road measurement of ammonia and other motor vehicle exhaust emissions, Environ. Sci. Technol., 34, 3535-3539,

doi:10.1021/es991451q, 2000.

Kean, A. J., Littlejohn, D., Ban-Weiss, G. A., Harley, R. A., Kirchstetter, T. W., and Lunden, M. M.: Trends in on-road vehicle emissions of ammonia, Atmos. Environ., 43, 1565-1570, doi: 10.1016/j.atmosenv.2008.09.085, 2009.

Liu, T. Y., Wang, X. M., Wang, B. G., Ding, X., Deng, W., Lu, S. J., and Zhang, Y. L.: Emission factor of ammonia ($NH_3$) from on-road vehicles in China: tunnel tests in urban Guangzhou, Environ. Res. Lett., 9, 064027, doi:10.1088/1748-9326/9/6/064027, 2014.

Liu, Z. R., Hu, B., Wang, L. L., Wu, F. K., Gao, W. K., and Wang, Y. S.: Seasonal and diurnal variation in particulate matter ($PM_{10}$ and $PM_{2.5}$) at an urban site of Beijing: analyses from a 9-year study, Environ. Sci. Pollut. Res., 22, 627-642, doi:10.1007/s11356-014-3347-0, 2015.

Lu, Y. L., Song, S., Wang, R. S., Liu, Z. Y., Meng, J., Sweetman, A. J., Jenkins, A., Ferrier, R. C., Li, H., Luo, W., and Wang, T. Y.: Impacts of soil and water pollution on food safety and health risks in China, Environ. Int., 77, 5-15, doi:10.1016/j.envint.2014.12.010, 2015.

Meng, Z. Y., Lin, W. L., Jiang, X. M., Yan, P., Wang, Y., Zhang, Y. M., Jia, X. F., and Yu, X. L.: Characteristics of atmospheric ammonia over Beijing, China, Atmos. Chem. Phys., 11, 6139-6151, doi:10.5194/acp-11-6139-2011, 2011.

MEPC (Ministry of Environmental Protection of the People's Republic of China): Ambient air quality standards (GB3095–2012), Available at: http://www.mep.gov.cn/ (accessed 29 February 2012).

Parrish, D. D., Singh, H. B., Molina, L., and Madronich, S.: Air quality progress in North American megacities: a review, Atmos. Environ., 45, 7015-7025, doi:10.1016/j.atmosenv.2011.09.039, 2011.

Peel, J. L., Klein, M., Flanders, W. D., Mulholland, J. A., Tolbert, P. E., and Committee, H. H. R.: Impact of improved air quality during the 1996 summer Olympic games in Atlanta on multiple cardiovascular and respiratory outcomes, Research Report, 148, 3-23, discussion 25-33, 2010.

Reche, C., Viana, M., Pandolfi, M., Alastuey, A., Moreno, T., Amato, F., Ripoll, A., and Querol, X.: Urban $NH_3$ levels and sources in a Mediterranean environment, Atmos. Environ., 57, 153-164, doi:10.1016/j.atmosenv.2012.04.021, 2012.

Shen, J. L., Tang, A. H., Liu, X. J., Kopsch, J., Fangmeier, A., Goulding, K., and Zhang, F. S.: Impacts of pollution controls on air Quality in Beijing during the 2008 Olympic Games, J. Environ. Qual., 40, 37-45, doi:10.2134/jeq2010.0360, 2011.

Song, W., Chang, Y. H., Liu, X. J., Li, K. H., Gong, Y, M., He, G. X., Wang, X. L., Christie, P., Zheng, M., Dore, A. J., and Tian, C. Y.: A multiyear assessment of air quality benefits from China's emerging shale gas revolution: Urumqi as a case study, Environ. Sci. Technol., 49, 2066-2072, doi:10.1021/es5050024, 2015.

Sun, Y. L., Zhuang, G. S., Tang, A. H., Wang, Y., and An, Z. H.: Chemical Characteristics of $PM_{2.5}$ and $PM_{10}$ in haze-fog episodes in Beijing, Environ. Sci. Technol., 40, 3148-3155, doi:10.1021/es051533g, 2006.

Sun, Y. L., Wang, Z. F., Du, W., Zhang, Q., Wang, Q. Q., Fu, P. Q., Pan, X. L., Li, J., Jayne, J., and Worsnop, D. R.: Long-term real-time measurements of aerosol particle composition in Beijing, China: seasonal variations, meteorological effects, and source analysis, Atmos. Chem. Phys., 15, 10149-10165, doi:10.5194/acp-15-10149-2015, 2015.

Sun, Y. L., Wang, Z. F., Wild, O., Xu, W. Q., Chen, C., Fu, P. Q., Du, W., Zhou, L.B ., Zhang, Q., Han, T. T., Wang, Q. Q., Pan, X. L., Zheng, H. T., Li, J., Guo, X. F., Liu, J. G., and Worsnop, D. R.: "APEC Blue": Secondary aerosol reductions from emission controls in Beijing, Sci. Rep., 6, 20668, doi: 10.1038/srep20668, 2016.

Tang, G., Zhu, X, Hu, B., Xin, J., Wang, L., Münkel, C., Mao, G., and Wang, Y.: Impact of emission controls on air quality in Beijing during APEC 2014: lidarceilometer observations, Atmos. Chem. Phys., 15, 12667-12680, doi:10.5194/acp-15-12667-2015, 2015.

Tao, Y., Yin, Z., Ye, X. N., Ma, Z., and Che, J. M.: Size distribution of

water-soluble inorganic ions in urban aerosols in Shanghai, Atmos. Pollut. Res., 5, 639-647, doi:10.5094/APR.2014.073, 2014.

Tian, Q. W., and Brimblecombe, P.: Managing air in Olympic cities, American Journal of Environmental Sciences, 4, 439-444, 2008.

Wang, S. X., Xing, J., Zhao, B., Jang, C., Hao, J. M. Effectiveness of national air pollution control policies on the air quality in metropolitan areas of China. J. Environ. Sci., 26, 13-22, doi: 10.1016/S1001-0742(13)60381-2, 2014.

Wang, T., Nie, W., Gao, J., Xue, L. K., Gao, X. M., Wang, X. F., Qiu, J., Poon, C. N., Meinardi, S., Blake, D., Wang, S. L., Ding, A. J., Chai, F. H., Zhang, Q. Z., and Wang, W. X.: Air quality during the 2008 Beijing Olympics: secondary pollutants and regional impact, Atmos. Chemis. Phys., 10, 7603-7615, doi:10.5194/acp-10-7603-2010, 2010.

Wang, W. T., Primbs, T., Tao, S., and Simonich, S. L. M.: Atmospheric Particulate Matter Pollution during the 2008 Beijing Olympics, Environ Sci Technol., 43, 5314-5320, 2009.

Wang, Y., Zhuang, G., Tang, A., Yuan, H., Sun, Y., Chen, S., and Zheng, A.: The ion chemistry of $PM_{2.5}$ aerosol in Beijing, Atmos. Environ., 39, 3771-3784, doi:10.1016/j.atmosenv.2005.03.013, 2005.

Xu, W., Zheng, K., Liu, X. J., Meng, L. M., Huaitalla, M. R., Shen, J. L., Hartung, E., Gallmann, E., Roelcke, M., and Zhang, F. S.: Atmospheric $NH_3$ dynamics at a typical pig farm in China and their implications, Atmos. Pollut. Res., 5, 455-463, doi:10.5094/APR.2014.053, 2014.

Xu, W., Luo, X. S., Pan, Y. P., Zhang, L., Tang, A. H., Shen, J. L., Zhang, Y., Li, K. H., Wu, Q. H., Yang, D. W., Zhang, Y. Y., Xue, J., Li, W. Q., Li, Q. Q., Tang, L., Lu, S. H., Liang, T., Tong, Y. A., Liu, P., Zhang, Q., Xiong, Z. Q., Shi, X. J., Wu, L. H., Shi, W. Q., Tian, K., Zhong, X. H., Shi, K., Tang, Q. Y., Zhang, L. J., Huang, J. L., He, C. E., Kuang, F. H., Zhu, B., Liu, H., Jin, X., Xin, Y. J., Shi, X. K., Du, E. Z., Dore, A. J., Tang, S., Collett, J. L., Goulding, K., Sun, Y. X., Ren, J., Zhang, F. S., and Liu, X. J.: 2015. Quantifying atmospheric nitrogen deposition

through a nationwide monitoring network across China. Atmos. Chem. Phys, 15, 12345-12360, doi:10.5194/acp-15-12345-2015, 2015.

Xu, W., Wu, Q. H., Liu, X. J., Tang, A. H., Dore, A. J., and Heal, M. R.: Characteristics of ammonia, acid gases, and $PM_{2.5}$ for three typical land-use types in the North China Plain, Environ. Sci. Pollut. Res., 23, 1158-1172, doi:10.1007/s11356-015-5648-3, 2016.

Yoo, J. M., Lee, Y. R., Kim, D., Jeong, M. J., Stockwell, W. R., Kundu, P. K., Oh, S. M., Shin, D. B., Lee, S. J. New indices for wet scavenging of air pollutants ($O_3$, CO, $NO_2$, $SO_2$, and $PM_{10}$) by summertime rain. Atmos. Environ., 82, 226-237, doi:10.1016/j.atmosenv.2013.10.022, 2014.

Zhang, L., Liu, L. C., Zhao, Y. H., Gong, S. L., Zhang, X. Y., Henze, D. K., Capps, S. L., Fu, T. M., Zhang, Q., and Wang, Y. X.: Source attribution of particulate matter pollution over North China with the adjoint method, Environ. Res. Lett., 10, 084011, doi:10.1088/1748-9326/10/8/084011, 2015.

Zhang, Q., Streets, D. G., Carmichael, G. R., He, K. B., Huo, H., Kannari, A., Klimont, Z., Park, I. S., Reddy, S., Fu, J. S., Chen, D., Duan, L., Lei, Y., Wang, L. T., and Yao, Z. L.: Asian emissions in 2006 for the NASA INTEX-B mission. Atmos. Chem. Phys., 9, 5131-5153, 2009.

Zhang, T., Cao, J. J., Tie, X. X., Shen, Z. X., Liu, S. X., Ding, H., Han, Y. M., Wang, G. H., Ho, K. F., Qiang, J., and Li, W. T.: Water-soluble ions in atmospheric aerosols measured in Xi'an, China: seasonal variations and sources, Atmos. Res., 102, 110-119, doi:10.1016/j.atmosres.2011.06.014, 2011.

Zhang, Y., Dore, A. J., Ma, L., Liu, X. J., Ma, W. Q., Cape, J. N., and Zhang, F. S.: Agricultural ammonia emissions inventory and spatial distribution in the North China Plain, Environ. Pollut., 158, 490-501, doi:10.1016/j.envpol.2009.08.033, 2010.

Zhang, Y. L., and Cao, F.: Fine particulate matter ($PM_{2.5}$) in China at a city level. Sci. Rep., 5, 14884, doi:10.1038/srep14884, 2015.

Zhao, B., Wang, P., Ma, J. Z., Zhu, S., Pozzer, A., and Li, W.: A high-resolution

Atmos. Chem. Phys. Discuss., doi:10.5194/acp-2016-591, 2016
Manuscript under review for journal Atmos. Chem. Phys.
Published: 5 September 2016


emission inventory of primary pollutants for the Huabei region, China, Atmos. Chem. Phys., 12, 481-501, doi:10.5194/acp-12-481-2012, 2012.

Atmos. Chem. Phys. Discuss., doi:10.5194/acp-2016-591, 2016
Manuscript under review for journal Atmos. Chem. Phys.
Published: 5 September 2016


**Figure captions**

**Fig. 1**. Maps showing the thirty-one monitoring sites, the Beijing municipality (the areas within the blue line, and the surrounding regions. Also shown are locations of Tiananmen, and the 3rd, 4th, 5th and 6th ring roads.

**Fig. 2**. Concentrations of $NH_3$ (**A**) and $NO_2$ (**B**) during the monitoring periods at different observation scales: concentrations at 31 ($NH_3$) or 17 ($NO_2$) sites (a), averaged concentrations for the sites within the 6th ring road (SWR), outside the 6th ring road but in Beijing (SOI) and outside Beijing (SOB) (b), averaged concentrations for the sites on the 3rd, 4th and/or 5th ring roads and non-road sites (NRS) (c).

**Fig. 3**. Comparison of $PM_{2.5}$, $PM_{10}$, $NO_2$, $SO_2$ and CO concentrations between the pre-Parade and Parade Blue periods at Beijing, cities in North China (excluding Beijing) and other cities in China (one asterisk on bars denotes significant difference at $p<0.05$, two asterisks on bars denote significant difference at $p<0.01$).

**Fig. 4**. 72-h backward trajectories for 100 m above ground level in Beijing city during the pre-Parade Blue period (1 to 19 August 2015) (a), the Parade Blue period (20 August to 3 September 2015) (b), and the post-Parade Blue period (4 to 30 September 2015) (c), and for sampling duration of $NH_3$ (8 to 19 September 2015) in the post-Parade Blue period (d).

**Fig. 5**. Daily values of AQI and daily ratios of CO to $SO_2$ concentrations and of $PM_{2.5}$ to CO concentrations in Beijing during the pre-Parade Blue and Parade Blue periods.

**Fig. 6**. Correlations between $NO_2$ and $NH_3$ concentrations measured on the 5th ring road in Beijing during the pre-Parade Blue, Parade Blue, and post-Parade Blue periods.

**Fig. 7**. Comparison of wind speed (WS), relative humidity (RH) and temperature (*T*) between the Parade Blue period and pre-Parade Blue period, and the post-Parade Blue period in Beijing, and between the Parade Blue and pre-Parade Blue periods in

North China (excluding Beijing) and other cities in China (two asterisk on bars denotes significant difference at $p<0.01$).

**Fig. 8**. 10 m mean wind field and (vector) and sea surface pressure (white) plotted on the precipitation field during the pre-Parade Blue period (left), Parade Blue period (right) and post-Parade Blue period (below).

**Fig. 9**. Mean sea level pressure (unit: hPa) and mean wind field at 10 m height (unit: m/s) during the pre-Parade Blue (a), Parade Blue (b) and post-Parade Blue (c) periods in Beijing and North China. The color bar denotes air pressure (unit: hPa) and arrows reflect wind vector (unit: m $s^{-1}$).

**Fig. 10**. The frequency distributions of wind directions and speeds (color demarcation) (a), and daily precipitation amount (b) in Beijing city during the pre-Parade Blue, Parade Blue, and post-Parade Blue periods.

**Fig. 11**. Dynamics of daily mean atmospheric mixing layer height (MLH) in Beijing from 3 August to 30 September 2015 (a) and comparison of MLH means during the pre-Parade Blue, Parade Blue and post-Parade Blue periods (b).

**Fig. 12**. Effect of meteorological condition change (MCC, simulated by a GEOS-Chem chemical transport model) and pollution control measures (PEM, measured by monitoring stations) to relative concentrations of CO, $NO_2$, $SO_2$, $NH_3$ and $PM_{2.5}$ (A) and relative contribution of MCC and PEC to major pollutant mitigation (B) in Beijing during the Parade Blue period.

**Fig. 13**. The correlations between emission reductions and air concentrations for (a) $PM_{2.5}$; (b) $PM_{10}$; (c) $NO_2$; and (d) $SO_2$.

Atmos. Chem. Phys. Discuss., doi:10.5194/acp-2016-591, 2016
Manuscript under review for journal Atmos. Chem. Phys.
Published: 5 September 2016


**Figure 1**

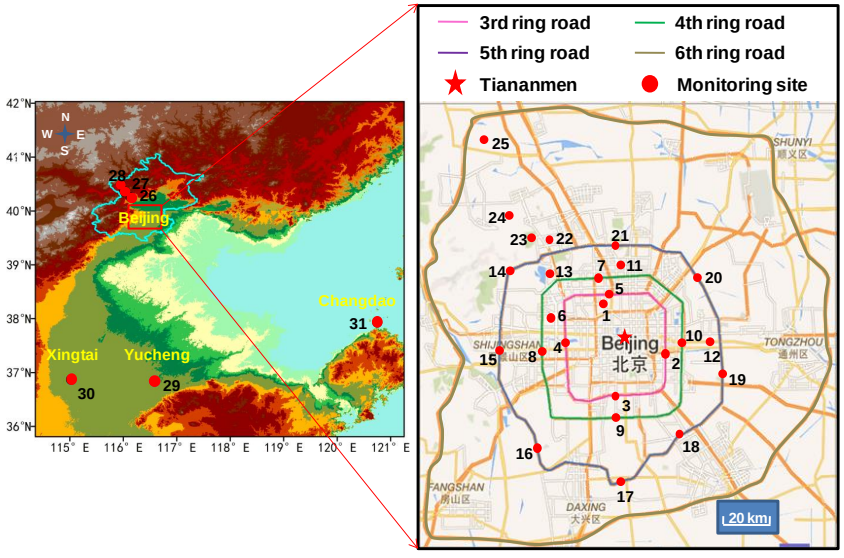

Atmos. Chem. Phys. Discuss., doi:10.5194/acp-2016-591, 2016
Manuscript under review for journal Atmos. Chem. Phys.
Published: 5 September 2016


**Figure 2**

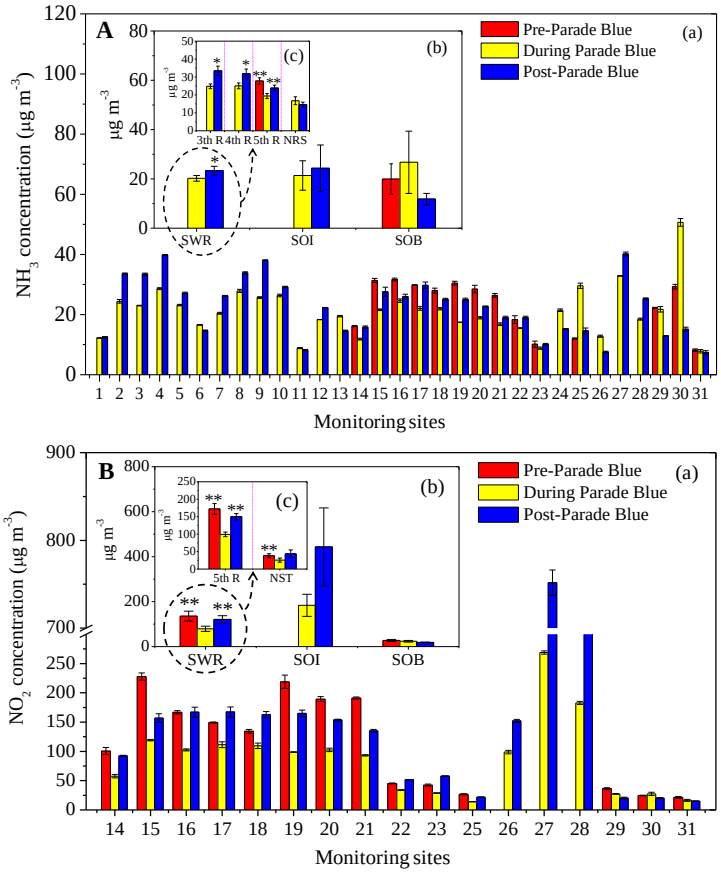

Atmos. Chem. Phys. Discuss., doi:10.5194/acp-2016-591, 2016
Manuscript under review for journal Atmos. Chem. Phys.
Published: 5 September 2016


**Figure 3**

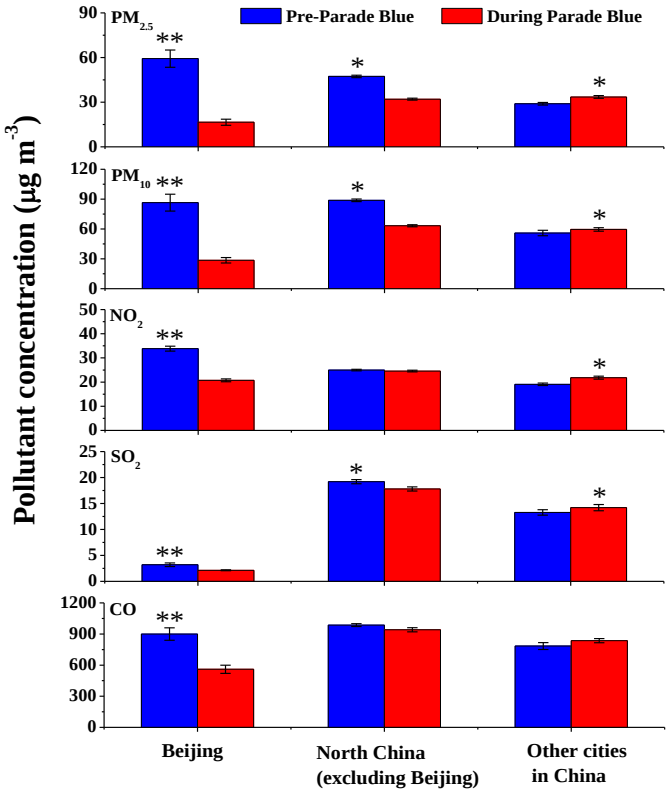

Atmos. Chem. Phys. Discuss., doi:10.5194/acp-2016-591, 2016
Manuscript under review for journal Atmos. Chem. Phys.
Published: 5 September 2016


**Figure 4**

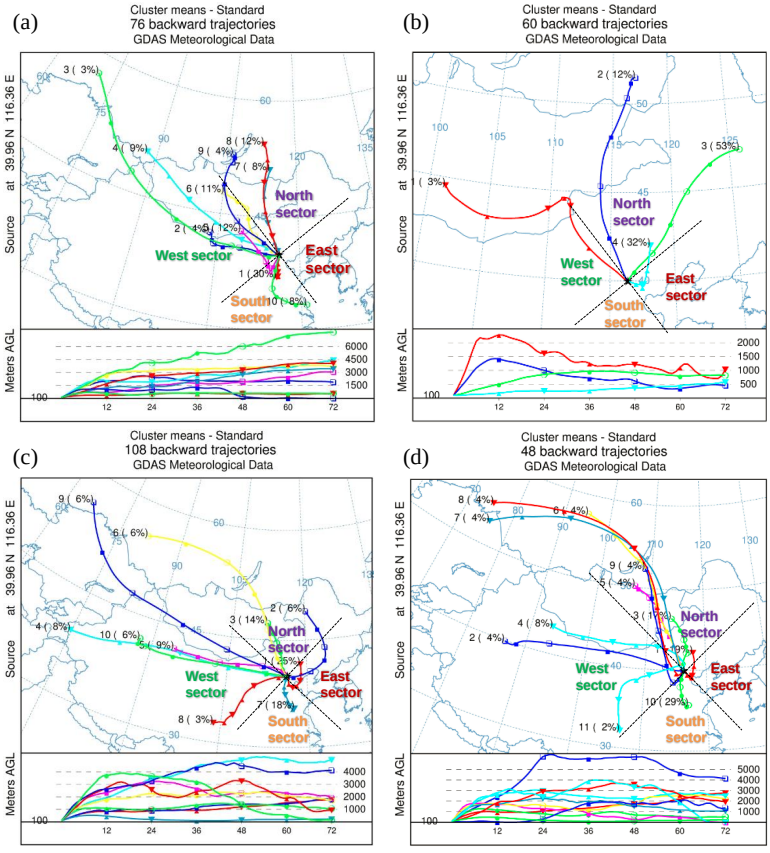

Atmos. Chem. Phys. Discuss., doi:10.5194/acp-2016-591, 2016
Manuscript under review for journal Atmos. Chem. Phys.
Published: 5 September 2016


**Figure 5**

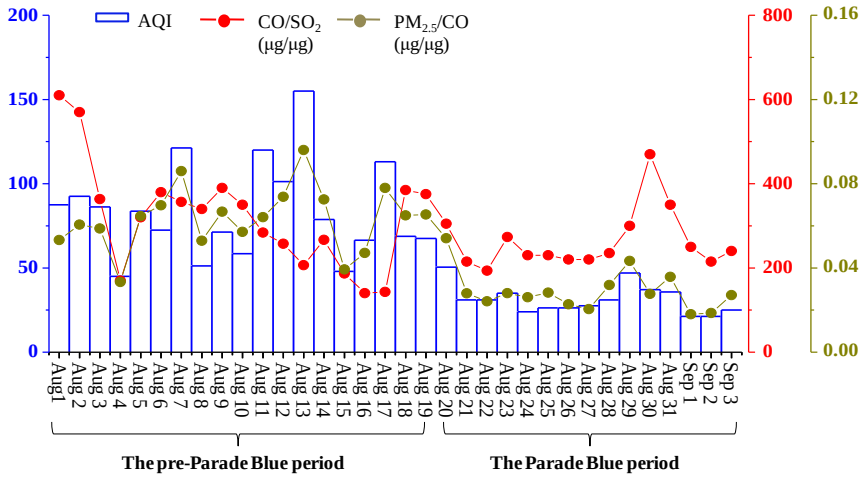

Atmos. Chem. Phys. Discuss., doi:10.5194/acp-2016-591, 2016
Manuscript under review for journal Atmos. Chem. Phys.
Published: 5 September 2016


**Figure 6**

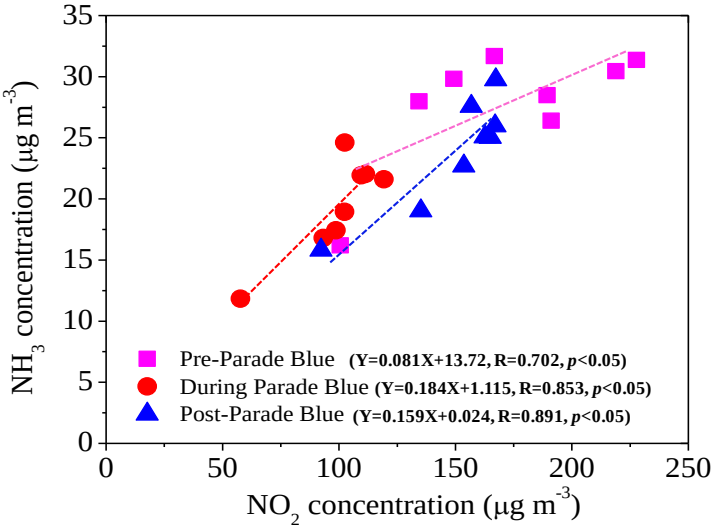

Atmos. Chem. Phys. Discuss., doi:10.5194/acp-2016-591, 2016
Manuscript under review for journal Atmos. Chem. Phys.
Published: 5 September 2016


**Figure 7**

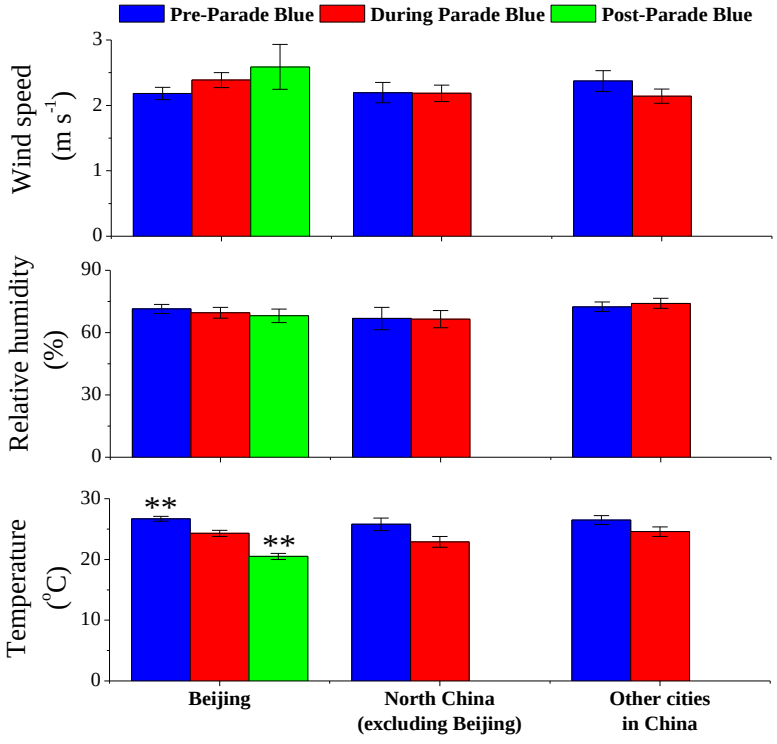

Atmos. Chem. Phys. Discuss., doi:10.5194/acp-2016-591, 2016
Manuscript under review for journal Atmos. Chem. Phys.
Published: 5 September 2016


**Figure 8**

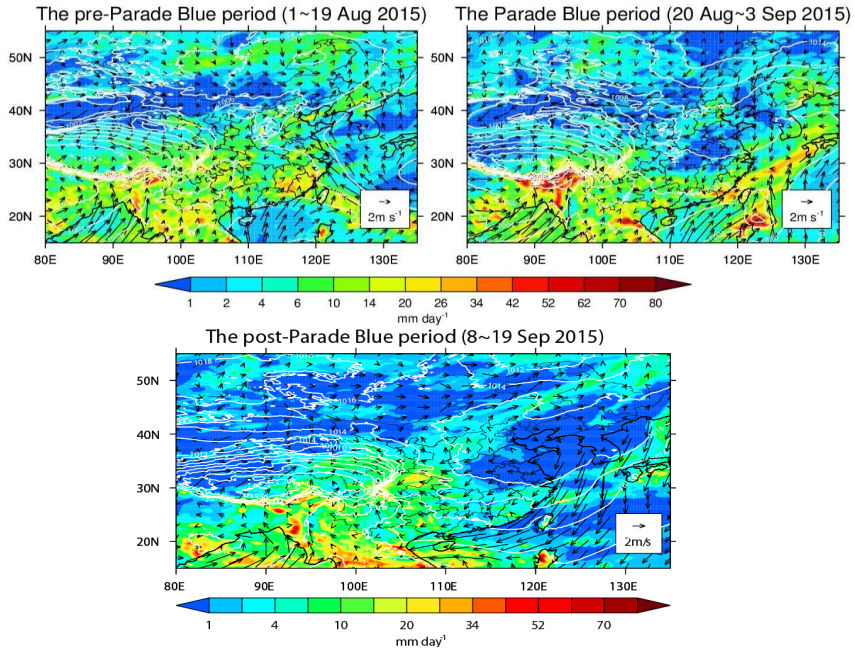

Atmos. Chem. Phys. Discuss., doi:10.5194/acp-2016-591, 2016
Manuscript under review for journal Atmos. Chem. Phys.
Published: 5 September 2016


**Figure 9**

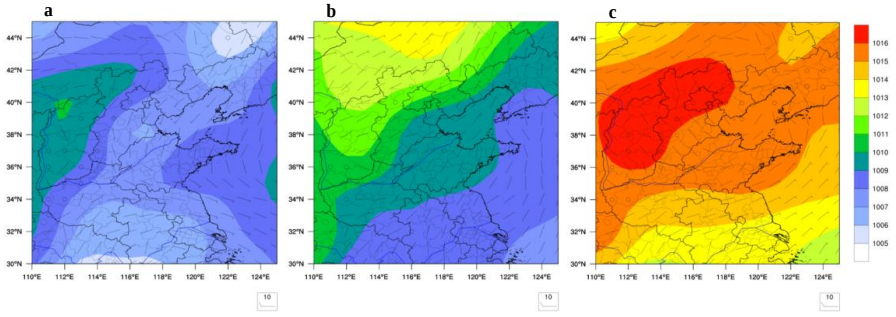

Atmos. Chem. Phys. Discuss., doi:10.5194/acp-2016-591, 2016
Manuscript under review for journal Atmos. Chem. Phys.
Published: 5 September 2016


**Figure 10**

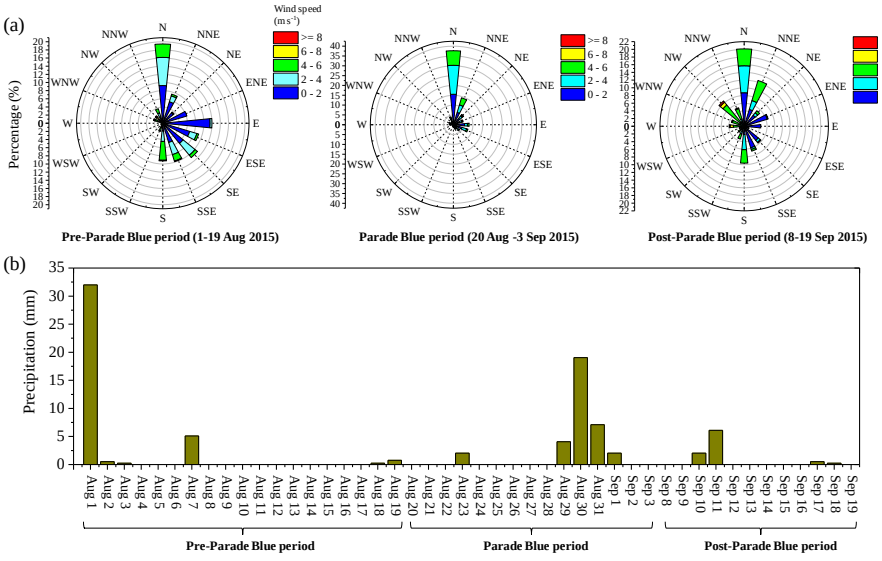

Atmos. Chem. Phys. Discuss., doi:10.5194/acp-2016-591, 2016
Manuscript under review for journal Atmos. Chem. Phys.
Published: 5 September 2016


**Figure 11**

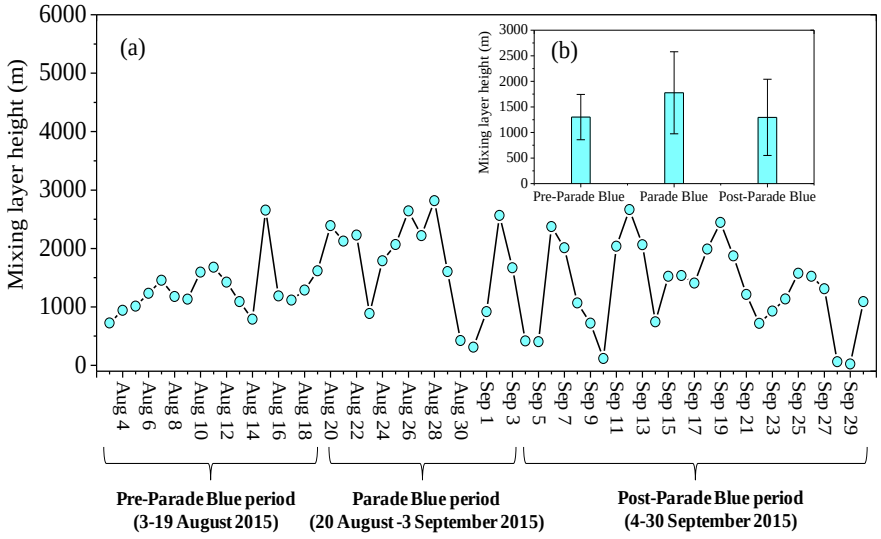

Atmos. Chem. Phys. Discuss., doi:10.5194/acp-2016-591, 2016
Manuscript under review for journal Atmos. Chem. Phys.
Published: 5 September 2016


**Figure 12**

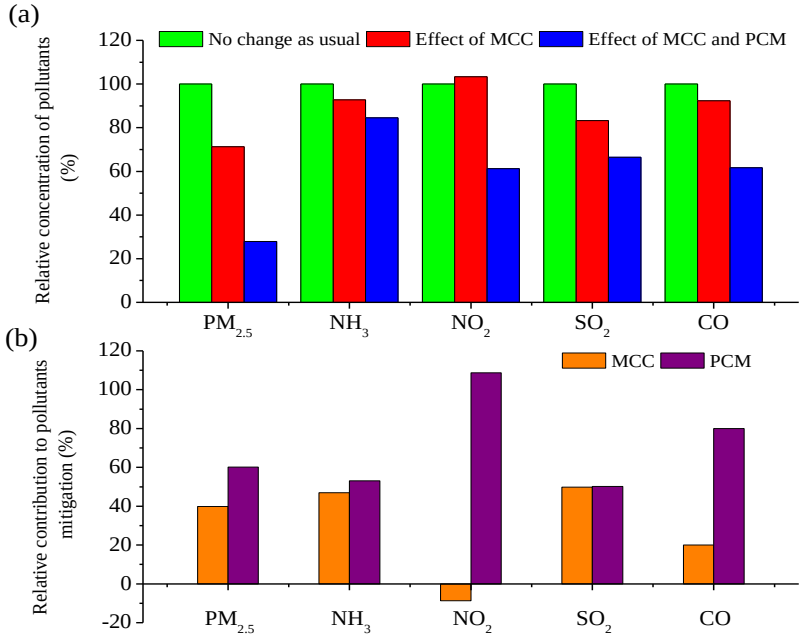

Atmos. Chem. Phys. Discuss., doi:10.5194/acp-2016-591, 2016
Manuscript under review for journal Atmos. Chem. Phys.
Published: 5 September 2016


**Figure 13**

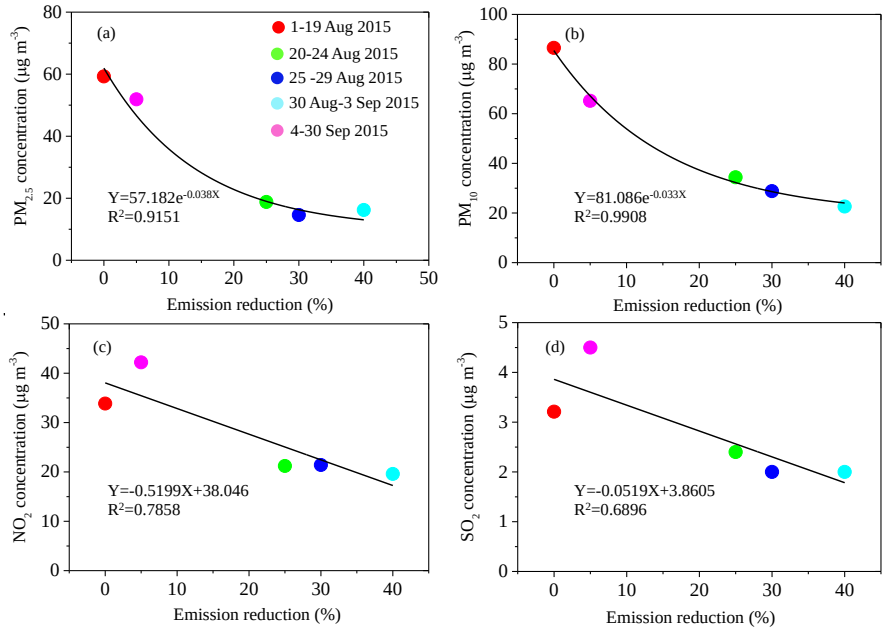

Atmos. Chem. Phys. Discuss., doi:10.5194/acp-2016-591, 2016
Manuscript under review for journal Atmos. Chem. Phys.
Published: 5 September 2016


**Table 1. Mean (SE) ambient concentrations of $PM_{2.5}$ and associated ionic components at the urban and rural sites.**

| | Urban site (Site 22) in Beijing | | | Rural site (Site 29) in Shandong | | | Rural site (Site 30) in Hebei | | |
|---|---|---|---|---|---|---|---|---|---|
| | Pre-PBP (n=11) | PBP[a] (n=15)[b] | Post-PBP (n=15) | Pre-PBP (n=6) | PBP (n=5) | Post-PBP (n=10) | Pre-PBP (n=6) | PBP (n=5) | Post-PBP (n=8) |
| $PM_{2.5}$ | 72.37 | 37.23 | 58.49 | 90.27 | 53.84 | 55.30 | 38.73 | 29.44 | 59.73 |
| | (7.36)** | (5.37) | (7.99) | (8.53)* | (11.37) | (7.45) | (5.17) | (6.55) | (16.35) |
| $NO_3^-$ | 2.07 | 0.85 | 6.27 | 4.21 | 1.22 | 5.56 | 0.58 | 1.02 | 3.46 |
| | (0.60) | (0.15) | (1.72)** | (1.71) | (0.22) | (1.03)** | (0.22) | (0.05) | (0.81)* |
| $SO_4^{2-}$ | 13.26 | 3.79 | 10.92 | 25.53 | 11.55 | 14.80 | 9.57 | 6.04 | 8.21 |
| | (2.85)** | (0.69) | (2.94) | (3.36)* | (3.20) | (2.84) | (1.07)* | 0.65 | 0.89 |
| $NH_4^+$ | 4.62 | 1.15 | 4.07 | 8.85 | 3.49 | 4.32 | 2.41 | 0.58 | 2.34 |
| | (0.94)** | (0.26) | (1.25) | (0.91)* | (1.01) | (0.98) | (0.30)** | 0.18 | (0.40)** |
| $Ca^{2+}$ | 0.58 | 0.38 | 0.51 | 0.29 | 0.29 | 0.23 | 0.19 | 0.12 | 0.09 |
| | (0.04)** | (0.06) | (0.07) | (0.06) | (0.11) | (0.05) | (0.07) | (0.02) | (0.02) |
| $K^+$ | 0.30 | 0.15 | 0.42 | 0.76 | 0.50 | 0.99 | 0.20 | 0.18 | 0.24 |
| | (0.04)** | (0.02) | (0.08)** | (0.07) | (0.11) | (0.18) | (0.03) | (0.02) | (0.02) |
| $F^-$ | 0.17 | 0.10 | 0.07 | 0.04 | 0.07 | 0.10 | 0.01 | 0.00 | 0.00 |
| | (0.02)* | (0.01) | (0.02) | (0.03) | (0.03) | (0.04) | (0.00) | (0.00) | (0.00) |
| $Cl^-$ | 0.11 | 0.11 | 0.13 | 0.14 | 0.29 | 0.19 | 0.06 | 0.01 | 0.24 |
| | (0.01) | (0.01) | (0.03) | (0.03) | (0.14) | (0.06) | (0.03) | (0.00) | (0.09)* |
| $Na^+$ | 0.10 | 0.09 | 0.25 | 0.25 | 0.45 | 0.42 | 0.35 | 0.52 | 0.26 |
| | (0.02) | (0.02) | (0.05)** | (0.05) | (0.25) | (0.04) | (0.08) | (0.06) | (0.02)** |
| $Mg^{2+}$ | 0.08 | 0.05 | 0.07 | 0.05 | 0.15 | 0.07 | 0.03 | 0.04 | 0.04 |
| | (0.01)** | (0.01) | (0.01) | (0.01) | (0.12) | (0.01) | (0.00)** | (0.00) | (0.00) |
| SIA[c] | 19.95 | 5.78 | 21.26 | 38.58 | 16.26 | 24.68 | 12.56 | 7.64 | 14.00 |
| | (3.83)** | (1.00) | (5.83)* | (3.75)** | (4.19) | (4.61) | (1.43)* | (0.81) | (1.97)* |
| $SIA/PM_{2.5}$ | 25.4 | 20.0 | 29.0 | 42.9 | 31.4 | 45.6 | 35.1 | 30.4 | 30.1 |
| (%) | (3.2) | (4.2) | (4.8) | (2.3) | (3.7) | (4.7) | (5.2) | (5.6) | (4.4) |

[a] Parade Blue period. [b] Number of samples. [c] Secondary inorganic aerosol.

*Significant at the 0.05 probability level. ** Significant at the 0.01 probability level.